PNAS
www.pnas.org

Supplementary Information for

Constitutive Dicer1 Phosphorylation accelerates metabolism and aging *in vivo*

Neeraj K Aryal, Vinod Pant, Amanda R Wasylishen, Jan Parker-Thornburg, Laura Baseler, Adel K. El-Naggar, Bin Liu, Awdhesh Kalia, Guillermina Lozano, Swathi Arur.

Email: gglozano@mdanderson.org, sarur@mdanderson.org

This PDF file includes:

Supplementary Figure and Legends

Figs. S1 to S6

www.pnas.org/cgi/doi/10.1073/pnas.1814377115

Figure S1:

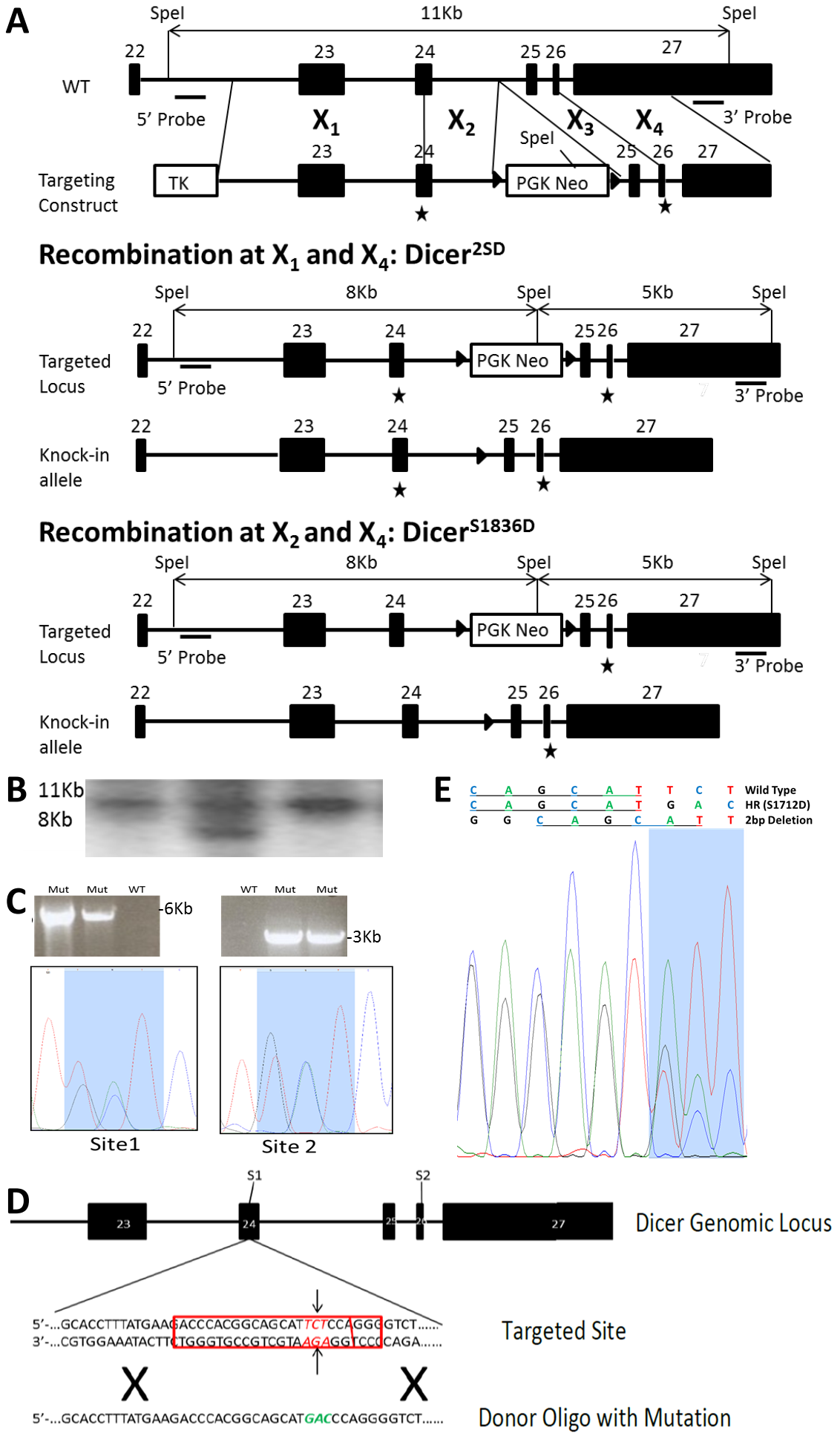
A
SpeI
11Kb
SpeI
22
23
24
25 26
27
WT
5' Probe
X1
X2
X3
X4
3' Probe
SpeI
23
24
25
26
27
Targeting Construct
TK
PGK Neo
Recombination at X1 and X4: Dicer2SD
SpeI
8Kb
SpeI
5Kb
SpeI
22
23
24
25 26
27
Targeted Locus
5' Probe
PGK Neo
3' Probe
Knock-in allele
Recombination at X2 and X4: DicerS1836D
B
11Kb
8Kb
C
Mut
Mut
WT
6Kb
WT
Mut
Mut
3Kb
Site1
Site 2
E
Wild Type
HR (S1712D)
2bp Deletion
D
S1
S2
23
24
27
Dicer Genomic Locus
5'-...GCACCTTTATGAAGACCCACGGCAGCATTCTCCAGGGGTCT.....
3'-...CGTGGAAATACTTCTGGGTGCCGTCGTAAGAGGTCCCCAGA.....
Targeted Site
X
X
5'-...GCACCTTTATGAAGACCCACGGCAGCATGACCCAGGGGTCT.....
Donor Oligo with Mutation

Generation of phospho-mimetic Dicer1 mouse models. A. DNA construct containing both mutations (S1836D and S1712D, marked by start symbol) was used to target endogenous Dicer1 locus in ES cells. Exes mark the possible recombination sites. SpeI restriction sites and expected size of DNA fragments are listed. **B**. Southern Blot using 5'-probe (see figure S1A) with 7.1Kb mutant band and 10.3Kb wild type DNA fragment. 8Kb and 11Kb markers (from DNA ladder) are shown. **C**. PCR based screening with one primer outside of targeted region and the other primer in the neo-R. Chromatographs from sequenced PCR fragment are shown. **D**. CRISPR/Cas9 based targeting to replace S1712 with aspartic acid in the endogenous Dicer1 locus of mouse zygote. **E**. Chromatographs from sequenced PCR fragment of mouse tail biopsy. Reverse primer was used for sequencing, and chromatograph is presented as reverse complement of the sequencing result.

Figure S2:

Dicer $^{+/S1712D}$ X *Dicer* $^{+/-}$				
Dicer $^{+/+}$	*Dicer* $^{+/-}$	*Dicer* $^{+/S1712D}$	*Dicer* $^{S1712D/-}$	P-value
6 (4.5)	3 (4.5)	5 (4.5)	4 (4.5)	0.77
Dicer $^{+/\Delta 1712}$ X *Dicer* $^{+/-}$				
Dicer $^{+/+}$	*Dicer* $^{+/-}$	*Dicer* $^{+/\Delta 1712}$	*Dicer* $^{\Delta 1712/-}$	P-value
5 (4)	4 (4)	4 (4)	3 (4)	0.91
Dicer $^{+/S1836D}$ X *Dicer* $^{+/-}$				
Dicer $^{+/+}$	*Dicer* $^{+/-}$	*Dicer* $^{+/S1836D}$	*Dicer* $^{S1836D/-}$	P-value
8 (6)	10 (6)	6 (6)	0 (6)	0.02
Dicer $^{+/2SD}$ X *Dicer* $^{+/-}$				
Dicer $^{+/+}$	*Dicer* $^{+/-}$	*Dicer* $^{+/2SD}$	*Dicer* $^{2SD/-}$	P-value
8 (5.5)	7 (5.5)	7 (5.5)	0 (5.5)	0.05

Dicer^{S1836D} and Dicer^{2SD} are hypomorphic alleles. Expected numbers are in parenthesis.

Figure S3:

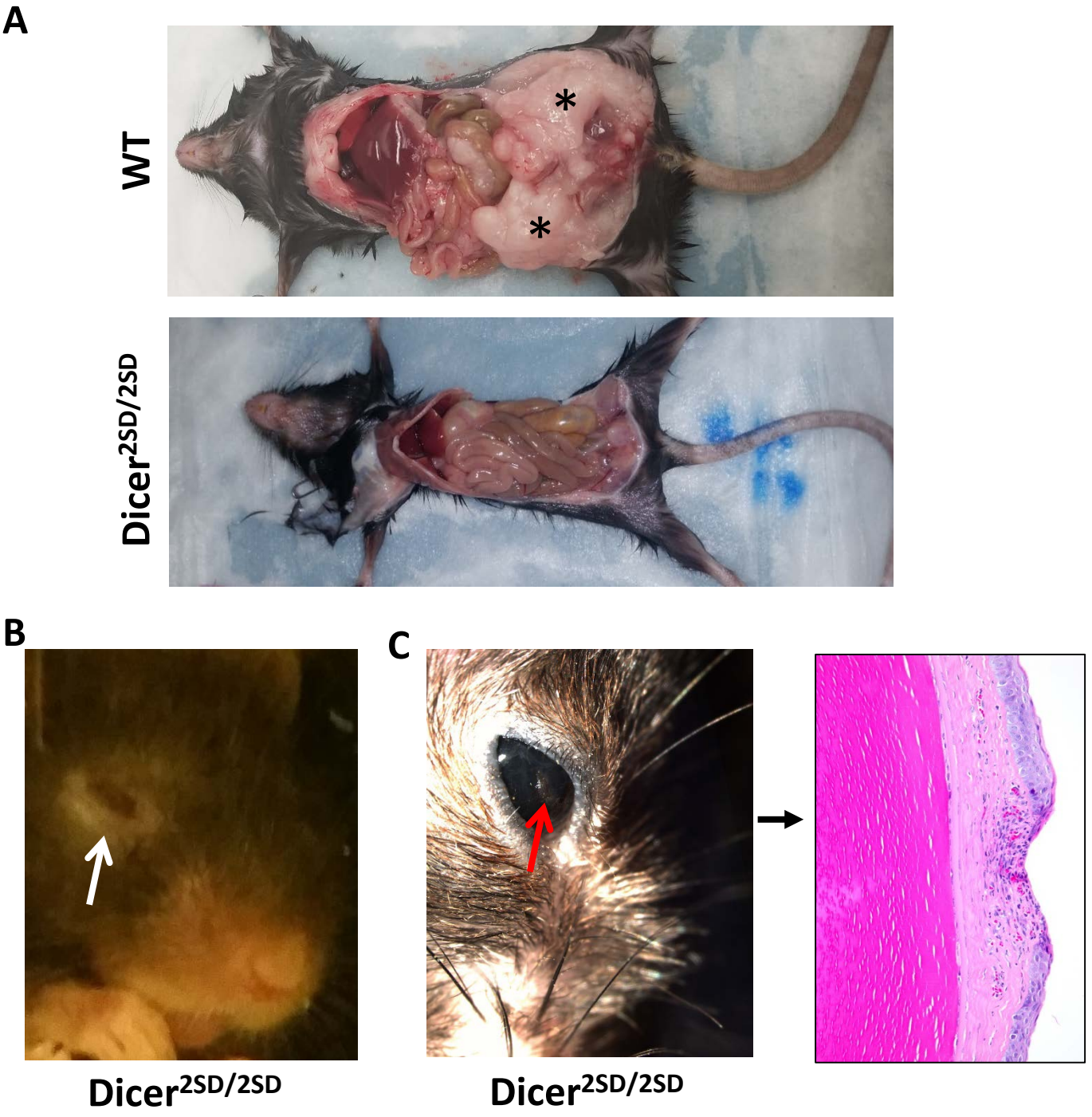

Loss of abdominal fat and development of ocular lesions in Dicer$^{2SD/2SD}$ mice . A. Representative images of ten month-old wild type and *Dicer$^{2SD/2SD}$* mouse showing visceral fat (asterisk). **B**. Representative image of neutrophilic conjunctivitis (arrow, white discoloration around the eyes) in a four month-old *Dicer$^{2SD/2SD}$* mouse. **C**. Macroscopic and microscopic images of a chronic corneal ulcer in an eight month-old *Dicer$^{2SD/2SD}$* mouse.

Figure S4:

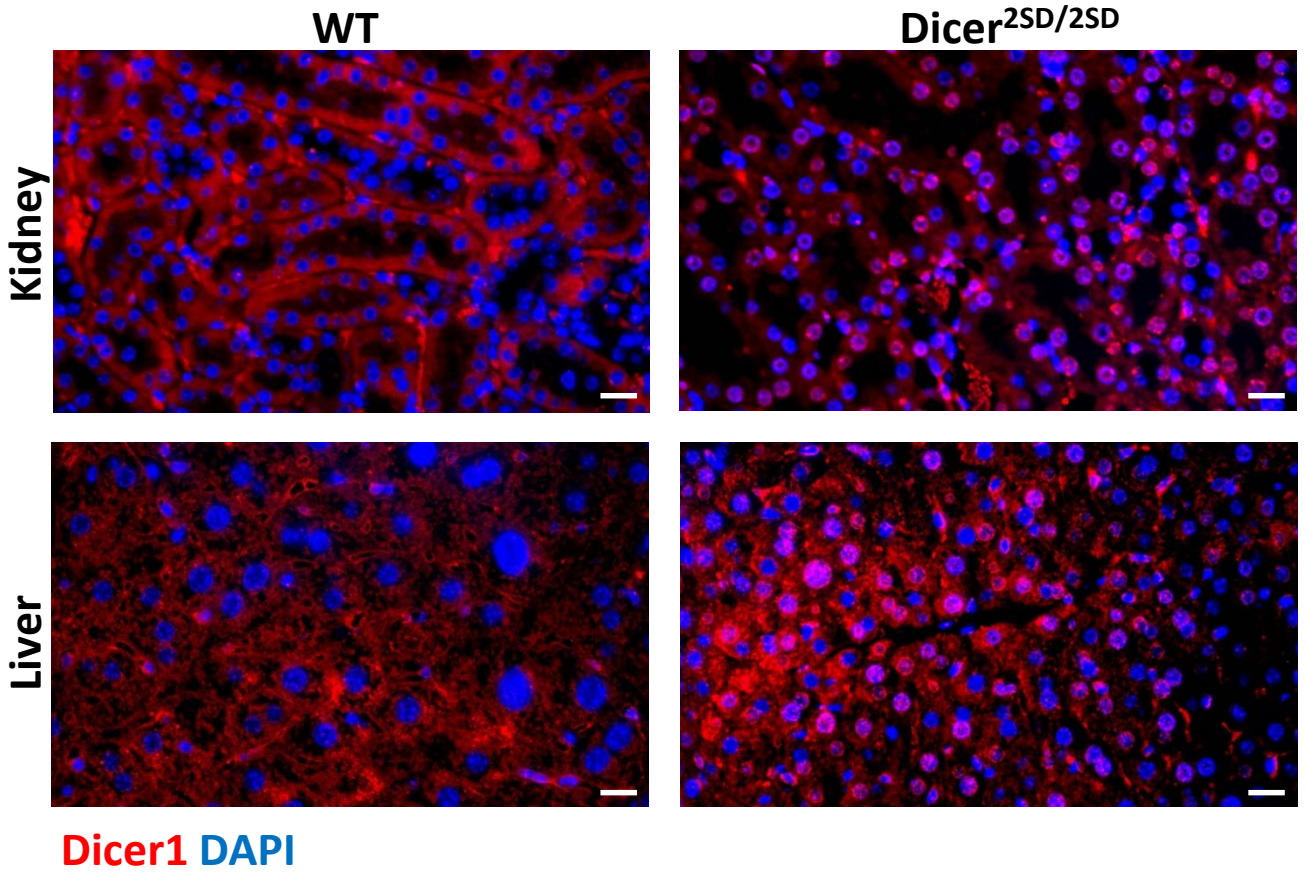

Dicer1 Localization. Immuno-fluorescence with anti-Dicer1 antibody (red) on representative kidney and liver sections from wild type (WT), and *Dicer*$^{2SD/2SD}$ mice. Scale bars = 20µm.

Figure S5:

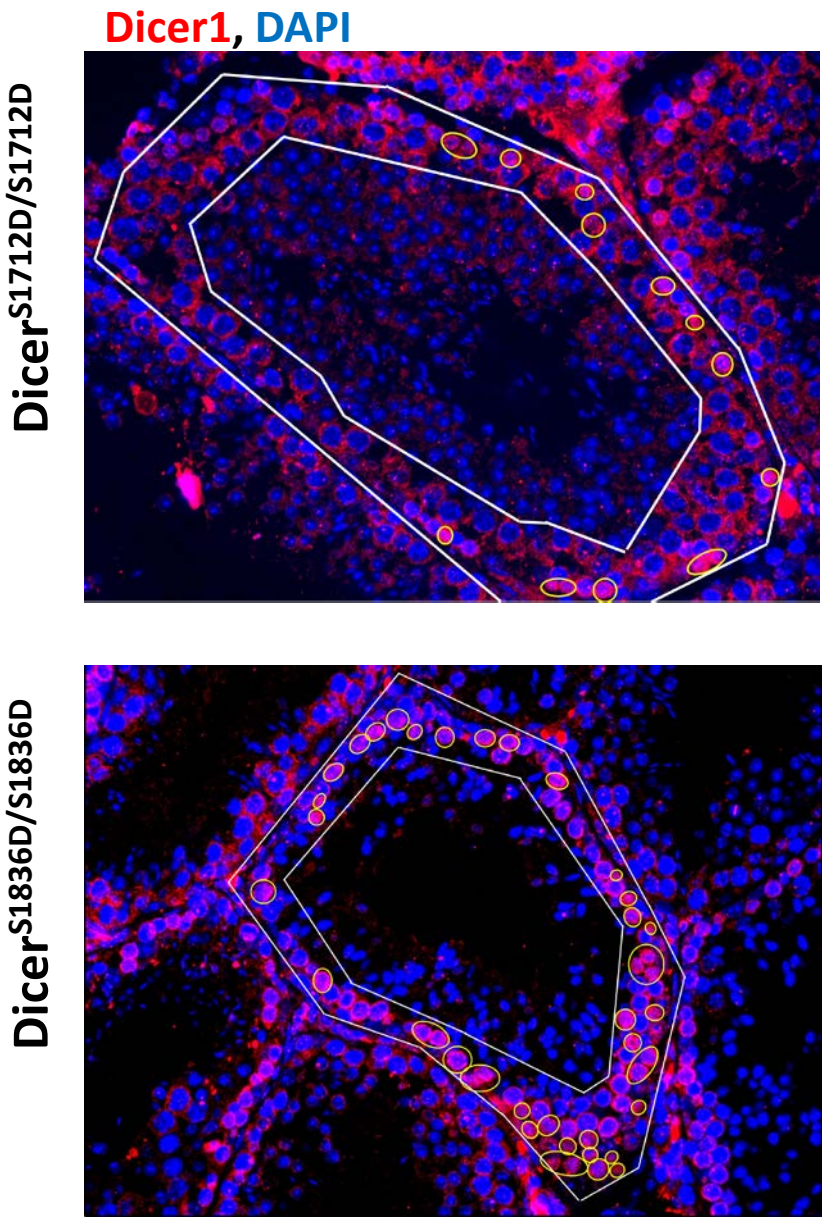

Quantification of spermatocytes with nuclear accumulation of Dicer1 Immuno-fluorescence with anti-Dicer1 antibody (red) on representative testes sections (20X) from *Dicer*$^{S1712D/S1712D}$ and *Dicer*$^{S1836D/S1836D}$ mice. Cells inside the white margins were included for quantification. Circled cells are counted as positive for nuclear accumulation. Cells with nuclear signal in >50% of nuclear surface (visually determined) were considered positive for nuclear accumulation.

Figure S6:

#	KEGG Pathway	P-value
1	Prion disease	2.5515e-10
2	Fatty acid biosynthesis	1.3331e-09
3	Fatty acid metabolism	4.2871e-09
4	Proteoglycans in cancer	4.6287e-07
5	Renal cell carcinoma	1.9558e-05
6	Thyroid hormone signaling pathway	2.8087e-05
7	Protein processing in endoplasmic reticulum	8.2850e-05
8	Axon guidance	8.4420e-05
9	N-Glycan biosynthesis	9.3190e-05
10	Long-term potentiation	0.0001
11	TGF-beta signaling pathway	0.0002
12	Lysine degradation	0.0004
13	T cell receptor signaling pathway	0.0005
14	Hippo signaling pathway	0.0005
15	FoxO signaling pathway	0.0010
16	Fatty acid elongation	0.0011
17	Phosphatidylinositol signaling system	0.0019
18	Long-term depression	0.0019
19	Ubiquitin mediated proteolysis	0.0027
20	Pathways in cancer	0.0027
21	MAPK signaling pathway	0.0051
22	Endocytosis	0.0059
23	Wnt signaling pathway	0.0059
24	Adherens junction	0.0082
25	Gap junction	0.0094

Pathway analysis of downregulated miRNAs in Dicer$^{2SD/2SD}$ MEFs